Multimodality imaging studies of intraductal tubulopapillary neoplasms of the pancreas

Hye Jin Kim ⓘ
Mi-Suk Park ⓘ
Taek Chung ⓘ
Bohyun Kim ⓘ
Jei Hee Lee ⓘ
Jai Keun Kim ⓘ

PURPOSE
We aimed to investigate multimodality imaging findings of intraductal tubulopapillary neoplasms (ITPN) of the pancreas.

METHODS
This study was approved by the institutional review board with waived informed consent. A total of eight patients were histopathologically diagnosed with pancreatic ITPN in a single institution over a 6-year period. The imaging findings of dynamic contrast-enhanced computed tomography (CT), magnetic resonance cholangiopancreatography (MRCP), endoscopic ultrasonography (EUS), and positron emission tomography-computed tomography (PET-CT) were reviewed and correlated with clinicopathologic findings.

RESULTS
Histopathologically, an invasive carcinoma component was found in 5 of 8 patients (62.5%). The median diameter of the lesions and the main pancreatic ducts were larger in ITPN with invasive carcinoma (19 mm, 13.3–98.0 mm and 13 mm, 5.9–16.3 mm, respectively) than in ITPN without invasive carcinoma (13 mm, 12.7–18.5 mm and 6 mm, 5.6–6.1 mm, respectively), but not significantly (lesions, $P = 0.229$ and main pancreatic ducts, $P = 0.143$). Pancreatolithiasis accompanied invasive carcinoma in 3 of 5 patients (60%). Intraductal solid tumors were demonstrated on CT (5/8, 62.5%), MRCP (5/7, 71.4%), and EUS (7/7, 100%). In addition, various imaging findings mimicking chronic autoimmune pancreatitis or pancreatic ductal adenocarcinoma were found in 3 patients (37.5%) on multimodality imaging. The lesion multiplicity and synchronous or metachronous biliary cancer occurred in 3 patients (37.5%), respectively.

CONCLUSION
Patients with associated invasive carcinoma from pancreatic ITPN may have presented a trend toward larger tumor size and dilated pancreatic duct with pancreatoliths, but the difference was not statistically significant. Further studies with a larger number of patients are needed to provide better insight into these findings. Pancreatic ITPN can show various atypical imaging findings as well as typical intraductal solid tumor on multimodality imaging. The presence of lesion multiplicity and synchronous or metachronous biliary cancer can be helpful for assisting with the diagnosis of pancreatic ITPN.

From the Department of Radiology (H.J.K., B.K., J.H.L., J.K.K.), Ajou University School of Medicine, Suwon, Korea; Departments of Radiology and Research Institute of Radiological Science (H.J.K., M.S.P. ✉ RADPMS@yuhs.ac) and Pathology (T.C.), Severance Hospital, Yonsei University School of Medicine, Seoul, Korea.

I ntraductal tubulopapillary neoplasm (ITPN) of the pancreas is a relatively recently established intraductal neoplasm of the pancreas that was first described in 2009 by Yamaguchi et al. (1). According to the current 2010 WHO classification (2), pancreatic intraductal neoplasms are classified into two groups: intraductal papillary mucinous neoplasm (IPMN) and ITPN. These two neoplasms are pancreatic intraductal epithelial tumors with the potential for malignancy (3). Pancreatic ITPN is histopathologically defined as an intraductal tubule-forming epithelial neoplasm with high-grade dysplasia without overt mucin production, in contrast to pancreatic IPMN. However, the rarity of this disease, which constitutes only 3% of intraductal neoplasms of the pancreas, limits the availability of pancreatic ITPN for study (1). In recent years, several researchers have reported clinicopathologic and immunohistochemical analysis of pancreatic ITPN and the correlation between clinicopathologic features and surgical outcomes in patients with pancreatic ITPN (4–9).

With the application of advanced imaging techniques, pancreatic intraductal lesions are being detected at an enormously increasing rate, but the majority of these lesions belong to pancreatic IPMN. Imaging studies of pancreatic ITPN have been limited to clinical case reports except for one study suggesting "2-tone duct sign" and "cork-of-wine-bottle sign" as characteristic imaging findings of ITPN (10). However, to our knowledge, there has been no report evaluating the imaging findings of ITPN according to its invasiveness.

The aim of this study is to evaluate the imaging findings of pancreatic ITPN according to invasiveness using various imaging modalities.

Methods

Patients and imaging studies

This retrospective study was approved by our institutional review board (protocol no. 4-2018-0239) and the requirement for informed consent was waived. Between January 2012 and January 2017, 8 patients were histopathologically diagnosed with pancreatic ITPN in our institution. Clinical characteristics of these patients were collected and reviewed from the electronic medical records.

All 8 patients underwent multidetector computed tomography (CT) examinations with either a 16- or 64-channel CT scanner (Sensation 16 or 64; Siemens). After performing pre-contrast CT images, two-phase contrast-enhanced CT images were obtained with intravenous administration of nonionic contrast medium (Ultravist 300;

Schering). Pancreatic phase images were obtained at 18 s after the time of peak abdominal aortic enhancement calculated near the hepatic hilum, and portal venous phase images at 18 s after the end of the pancreatic phase. The scanning parameters were as follows: rotation time, 0.5 s; beam collimation, 0.75 and 0.625 mm; slice thickness, 5 and 3 mm; reconstruction interval, 5 and 3 mm; effective tube current-time charge, 150–250 mAs; 120 kVp for the 16- and 64-channel CT scanner, respectively.

Seven patients underwent magnetic resonance cholangiopancreatography (MRCP) with a 1.5 T (Intera Achieva; Philips Medical Systems) or 3.0 T (Magnetom Trio Tim; Siemens Medical Solutions) scanner with a 4- or 16-channel body coil. Pre-contrast magnetic resonance imaging (MRI) protocol consisted of breath-hold axial T1-weighted dual fast-gradient-recalled echo sequence and T2-weighted single- or multi-shot turbo spin-echo with spectral fat suppression. All two-dimensional (2D) and three-dimensional (3D) MRCP imaging was obtained with 2D thick-slab single-shot turbo spin-echo with a relaxation enhancement sequence and with 3D T2-weighted respiratory-triggered fast spin-echo sequence using a navigator technique. Contrast-enhanced dynamic T1-weighted imaging was obtained after administration of extracellular contrast agent as a bolus injection of 0.2 mL/kg gadoterate meglumine (Dotarem, Guerbet), followed by 20 mL saline flush using a power injector. The arterial phase began 5 s after the peak aortic enhancement was determined. Portal (50 s) and equilibrium (3 min) phase images were obtained after contrast agent administration, respectively. Diffusion-weighted imaging was performed using a navigator-triggered single-shot echoplanar sequence with b values of 0, 50, 400, and 800 s/mm^2. Imaging parameters for MRCP sequences are summarized in Table 1.

Seven patients underwent endoscopic ultrasonography (EUS) using an ultrasound scanner (EU-M30, Olympus) with 12 MHz transducers (GFUM-240; Olympus Optical Co) with variable frequencies of 5, 7.5, 12, and 20 MHz by an experienced gastroenterologist (16 years of experience).

Four patients underwent positron emission tomography-CT (PET-CT) (Discovery STE, GE Healthcare). After CT scan was performed from the skull base to the proximal thighs for attenuation purpose, PET scan was performed with an acquisition time of

3 min per bed position in 3D mode after injection of 5.5 MBq/kg of ^{18}F-fluorodeoxyglucose (^{18}F-FDG). The PET scans were reconstructed using ordered subset expectation maximization with attenuation correction.

Imaging analysis

CT and MRCP images were retrospectively evaluated in consensus by two board certified abdominal radiologists with 13 and 17 years of experience. The following imaging features were analyzed: location (head including uncinated process, body, or tail), size, extent (focal or diffuse), and presence of intraductal solid tumor, attenuation/signal intensity/echogenicity of solid nodule compared with those of the normal pancreatic parenchyma, main pancreatic duct dilatation, chronic pancreatitis, pancreatolithiasis, presence of diffusion restriction on MRI, and FDG uptake on PET-CT.

Statistical analysis

Statistical analyses were performed by one author using a commercial statistical software package (SPSS for Windows, version 23.0; IBM Corp.). The Mann-Whitney U test was used to evaluate differences between cancer and noncancer groups for continuous variables. All reported P values were two sided, and $P < 0.05$ was considered to be statistically significant.

Results

Clinical and pathologic characteristics of patients with pancreatic ITPN are summarized in Table 2. Five patients had symptoms of abdominal pain (n=4) or jaundice with elevated cancer antigen 19-9 level caused by synchronous bile duct cancer (n=1). Seven patients underwent surgical resection and one patient underwent biopsy for both pancreatic and hepatic lesions. One patient had synchronous triple primary biliary cancers of different histopathologic types: well-differentiated common bile duct (CBD) cancer; poorly differentiated ampulla of Vater cancer; and pancreatic ITPN associated with an invasive carcinoma. Three patients had metachronous gallbladder (n=2) and CBD (n=1) cancer.

Histopathologic analysis showed an invasive carcinoma component in 5 of 8 patients (62.5%). The maximal diameter of the pathologic specimens ranged from 1.3 to 8.0 cm (median, 2.5 cm).

Imaging characteristics of CT, MRCP, and EUS are summarized in Table 2. The lesions were located in the pancreatic head (n=3),

Table 1. MRI and MRCP imaging parameters

| Parameter | MRI sequence parameters | | | | | | |
	3D T1W GRE sequence	Dual-echo T1W GRE sequence	Respiratory-triggered TSE T2W sequence	Breath-hold HASTE T2W sequence	2D MRCP	3D MRCP	DWI
Imaging plane	Axial	Axial	Axial	Axial	Coronal	Coronal	Axial
Repetition time (ms)*	3.3/4.1	140/150	1900	400	8000	1600	2000
Echo time (ms)*	1.2/1.5	1.2/2.5	88	81	800	650	81
Flip angle (degrees)	9–13	65–70	150	150	90	90	90
Matrix	256×192	256×192	384×207	384×216	256×256	256×256	192×156
Field of view (mm²)	320×240–280	300×240–400	370×240–280	370×240–280	300×300	340×340	370×240–280
Received band width (kHz)	350	1028	260	766	383	318	1446
Section thickness (mm)	3–6	3–6	3–6	3–6	40	2	3–6
No. of signal acquisitions	1	1	2	1	1	2	5
Echo-train length	NA	1	13	256	256	87	122
Acceleration factor	2	2	2	2	0	4	2

MRI, magnetic resonance imaging; MRCP, magnetic resonance cholangiopancreatography; 3D, three-dimensional; 2D, two-dimensional; T1W, T1-weighted; T2W, T2-weighted; GRE, gradient-recalled echo; TSE, turbo-spin echo; HASTE, half-Fourier acquisition single-shot TSE; DWI, diffusion-weighted imaging; NA, not available.
*Repetition and echo times represent the respective values of the 1.5 and 3.0 T MRIs.

Table 2. Clinical, pathologic, and imaging characteristics of patients with pancreatic ITPN

| Case | Age/Sex | Pathologic diagnosis | Identifiable mass within the pancreatic duct | | | Lesion/P-duct diameter[a] | Elevated CA19-9[b] | Pancreatolith | Diffuse/ Multifocal lesions |
			CT	MRCP	EUS	CT or MRCP (mm)	(U/mL)		
1	47/M	ITPN with high-grade dysplasia	(-)	(-)	(+)	NA / 6.1	(-)	(-)	(+)
2	53/M	ITPN with high-grade dysplasia	(+)	(+)	(+)	18.5 & 13.3 / 5.6	(-)	(-)	(+)
3	65/M	ITPN with multifocal adenocarcinoma transformation	(-)	(-)	(+)	13.3 / 5.9	(-)	(-)	(-)
4	71/F	ITPN with an associated invasive carcinoma	(+)	NA	(+)	15.0 / 12.0	(+)	(-)	(-)
5	53/M	ITPN with an associated invasive carcinoma	(+)	(+)	NA	98.0 / 14.5	(-)	(+)	(-)
6	65/F	ITPN with an associated invasive carcinoma	(+)	(+)	(+)	23.1 / 13.0	(-)	(+)	(-)
7	50/F	ITPN with high-grade dysplasia	(-)	(+)	(+)	12.7 / 6.0	(-)	(-)	(-)
8	34/M	ITPN with an associated invasive carcinoma & hepatic metastases	(+)	(+)	(+)	NA / 16.3	(-)	(+)	(+)

ITPN, intraductal tubulopapillary neoplasm; P-duct, pancreatic duct; CA 19-9, cancer antigen 19-9; CT, computed tomography; MRCP, magnetic resonance cholangiopancreatography; EUS, endoscopic ultrasonography; M, male; F, female; (-), negative findings; (+), positive findings; NA, not available.
[a]The largest lesion and P-duct diameter were selected from either CT or MRI modalities.
[b]Elevated CA 19-9 level was defined as >37 U/mL.

body (n=2), head to body (n=1), and body to tail (n=2) (Fig. 1).

The median diameter of the lesions was 19 mm (13.3–98.0 mm) in ITPN with invasive carcinoma and 13 mm (12.7–18.5 mm) in ITPN without invasive carcinoma. The median diameter of the main pancreatic ducts was 13 mm (5.9–16.3 mm) in ITPN with invasive carcinoma and 6 mm (5.6–6.1 mm) in ITPN without invasive carcinoma. However, there was no significant difference in the median diameter of the lesions ($P = 0.229$) and the pancreatic ducts ($P = 0.143$) according to the invasiveness. Four of 5 (80%) patients with ITPN associated with invasive
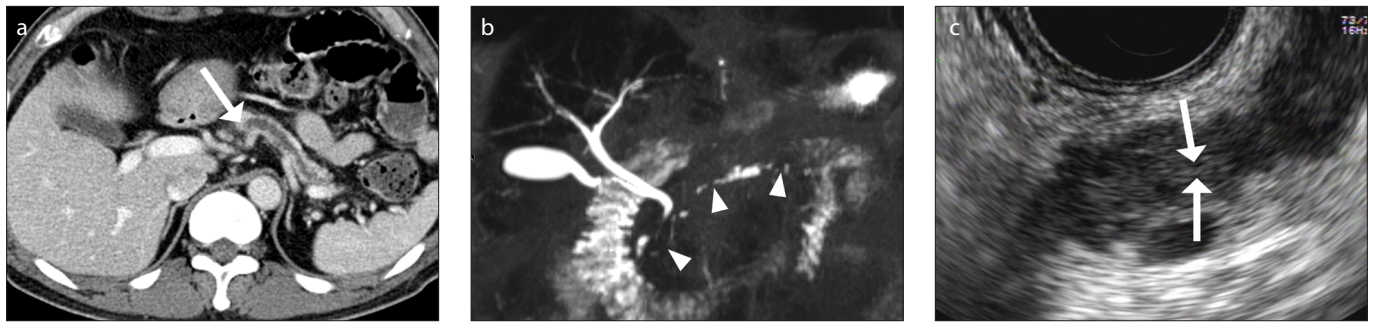
Figure 1. a–c. Case 1, a 47-year-old man with diffuse intraductal tubulopapillary neoplasm (ITPN). Axial contrast-enhanced portal phase CT image **(a)** shows abrupt cutoff *(arrow)* of the moderately dilated main pancreatic duct in the atrophied pancreas body. Three-dimensional magnetic resonance cholangiopancreatography (MRCP) image **(b)** shows diffuse irregular dilatation with stricture of the main pancreatic duct *(arrowheads)*. From CT and MRCP images, the presumptive radiologic diagnosis was chronic autoimmune pancreatitis. Repeated endoscopic ultrasonography (EUS) image **(c)** reveals a subtle isoechoic solid tumor *(arrows)* within the dilated main pancreatic duct. Positron emission tomography-CT (PET-CT) showed mild 18F-FDG uptake suggesting a benign inflammatory lesion rather than malignancy in the corresponding area (not seen).
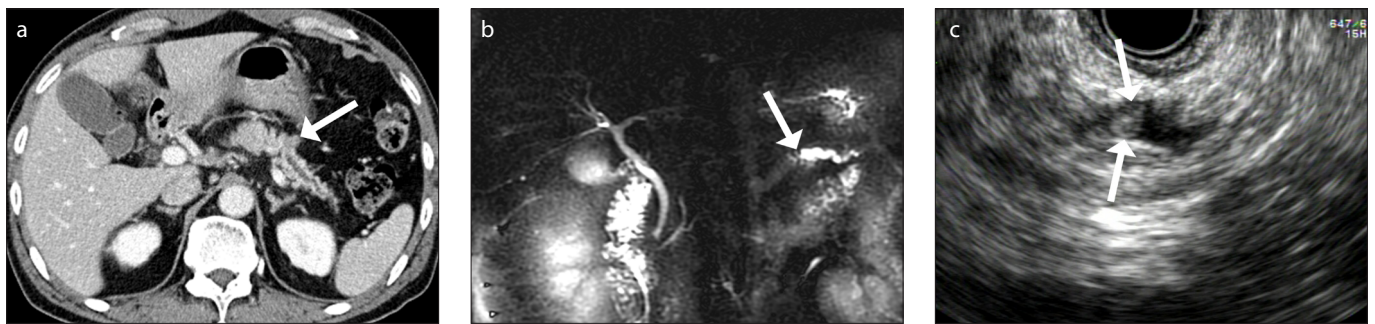

Figure 2. a–c. Case 3, a 65-year-old man with focal pancreatic ITPN with multifocal adenocarcinoma transformation. Axial contrast-enhanced portal phase CT image **(a)** shows a low attenuating nodular lesion *(arrow)* in the pancreas body with moderately dilated distal pancreatic duct. Two-dimensional MRCP image **(b)** shows abrupt cutoff *(arrow)* of the dilated main pancreatic duct in the pancreas body. EUS **(c)** reveals an intraductal tumor *(arrows)* within the dilated main pancreatic duct. The presumptive radiologic diagnosis was pancreatic ductal adenocarcinoma.
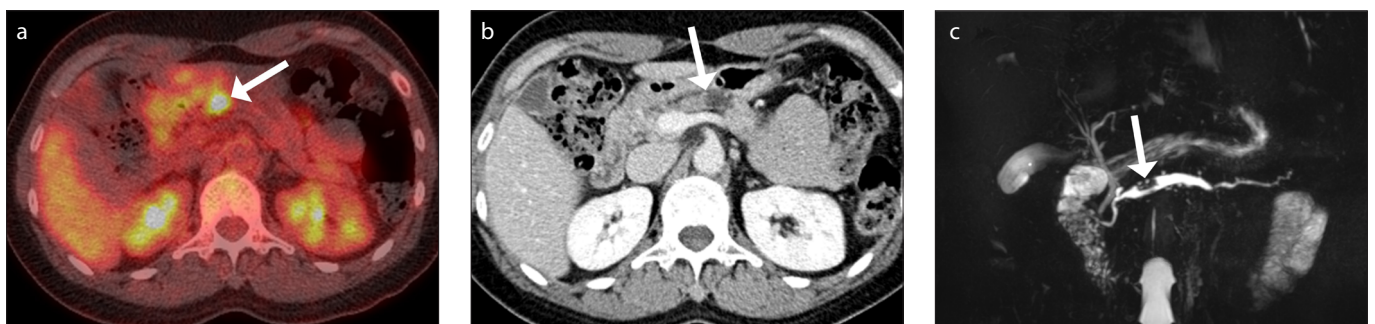

Figure 3. a–c. Case 7, a 50-year-old woman with focal pancreatic ITPN with high-grade dysplasia. PET-CT **(a)** performed for breast cancer work-up incidentally shows a focal strong 18F-FDG uptake *(arrow)* in the pancreas body. Axial contrast-enhanced portal phase CT image **(b)** shows only abrupt cutoff *(arrow)* of the moderately dilated main pancreatic duct in the pancreas body. Two-dimensional MRCP image **(c)** clearly shows an intraductal tumor *(arrow)* seen as a focal filling defect within the dilated main pancreatic duct.

carcinoma had pancreatic duct dilatation greater than 10 mm and 3 of 5 patients had impacted pancreatolithiasis. The 3 patients without invasive carcinoma did not have pancreatolithiasis.

Intraductal solid tumor within the main (n=7) or branch (n=1) pancreatic duct was detected in 62.5% of cases with CT (5 of 8), 71.4% with MRCP (5 of 7), and 100% with EUS (7 of 7). In two patients intraductal solid tumor was not detected on either CT and MRI, but was detected on EUS. One patient showed diffuse involvement of ITPN with irregular main pancreatic duct dilatation, mimicking chronic autoimmune pancreatitis on MRCP (Fig. 1). The other patient showed a small mass with upstream duct dilatation, which was preoperatively interpreted as pancreas cancer (Fig. 2). In one patient with invisible intraductal tumor at CT, MRCP demonstrated a small intraductal solid tumor with both upstream and downstream duct dilatation, similar to the "2-tone duct sign" (Fig. 3). In another patient, CT, MRCP, and EUS showed a large solid tumor within the cystic lesion and stones within the dilated duct in the pancreas head/uncinated process, mimicking branch duct type of IPMN with chronic pancreatitis (Fig. 4).

Compared with the adjacent pancreatic parenchyma, all of the solid tumors showed low or iso-enhancement on CT (n=6) (Fig. 5)
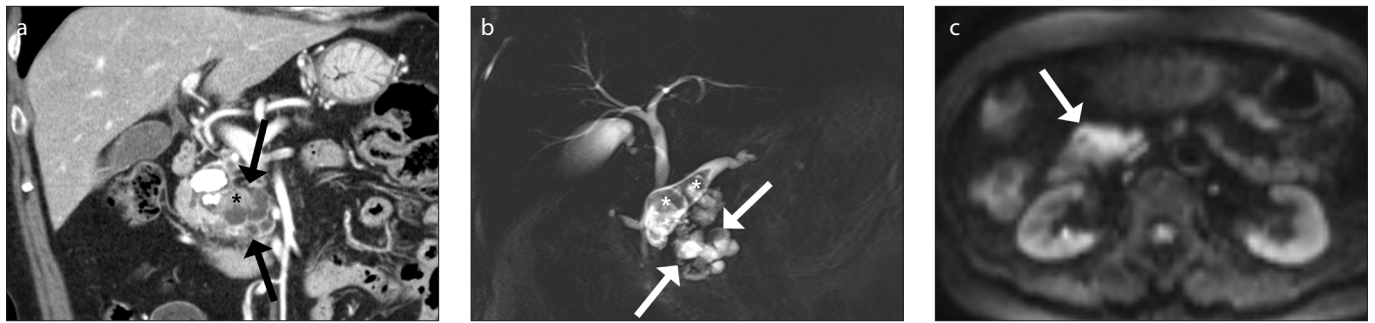
Figure 4. a–c. Case 6, a 65-year-old woman with focal pancreatic ITPN with invasive carcinoma. Coronal reconstructed contrast-enhanced portal phase CT image **(a)** shows a cystic lesion *(arrows)* in the pancreas head/uncinated process with intracystic low attenuating solid tumor *(asterisk)* as well as impacted pancreatoliths in the dilated main pancreatic duct. Two-dimensional MRCP image **(b)** shows a pleomorphic shaped cystic lesion with intracystic filling defect *(arrows)* suggesting solid tumor in the corresponding area as well as pancreatoliths *(asterisks)* with markedly dilated main pancreatic duct. Diffusion-weighted axial image **(c)** obtained at a *b* value of 800 reveals diffuse restriction *(arrow)* in the pancreas head/uncinated process. The presumptive radiologic diagnosis was branch duct type IPMN (intraductal papillary mucinous neoplasm) with chronic pancreatitis.
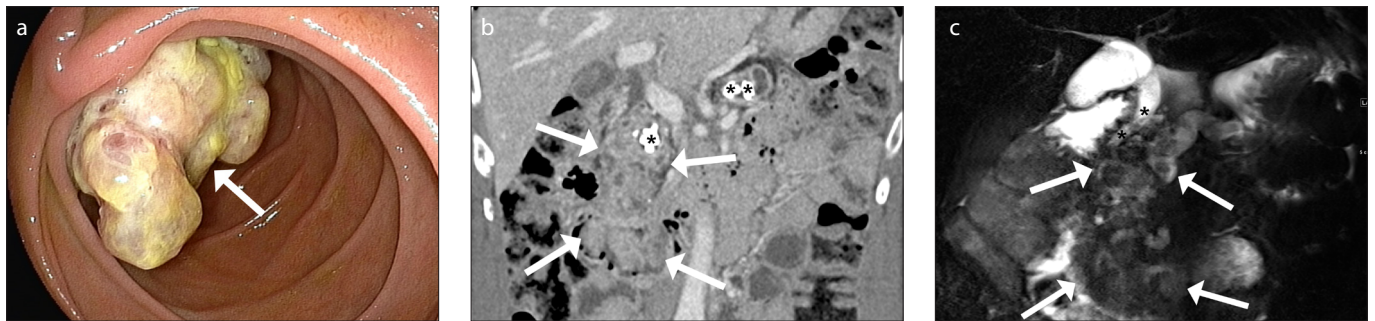

Figure 5. a–c. Case 5, a 53-year-old-man with focal pancreatic ITPN with invasive carcinoma. Esophagogastroduodenoscopy **(a)** performed for routine screening shows a large polypoid mass *(arrow)* in the duodenal 2nd portion. Coronal reconstructed contrast-enhanced portal phase CT image **(b)** shows a large polypoid isoattenuating mass *(arrows)* replacing the main pancreatic duct in the pancreas head with extension to the lumen of the duodenal 2nd portion. Several pancreatoliths *(asterisks)* are also intermingled with the mass or located in the markedly dilated distal pancreatic duct. Three-dimensional MRCP image **(c)** shows a large polypoid filling defect *(arrows)* along the dilated main pancreatic duct in the pancreas head and duodenal 2nd portion as well as displaced extrahepatic bile duct *(asterisks)*.

or MRI (n=7). All 8 patients were accompanied by chronic pancreatitis, which manifested as diffuse pancreatic parenchymal atrophy with or without pancreatoliths.

Among 7 patients undergoing MRI, diffusion restriction was found in 5, and 3 of these had ITPN with invasive carcinoma (Fig. 4c). Three patients with ITPN with high-grade dysplasia had focal mild to strong (Fig. 3a) FDG uptake on PET-CT, whereas one patient with invasive carcinoma had no FDG uptake.

Discussion

Pancreatic ITPN is a very rare and relatively slowly growing intraductal pancreatic tumor. According to previously published literature, pancreatic ITPN has a favorable clinical outcome with overall 5-year survival rate greater than 70% to 80% regardless of an invasive carcinoma component (6, 7). Therefore, there has been an effort to differentiate ITPN from other intraductal pancreatic lesions such as IPMN or pancreatic

ductal adenocarcinoma with a focus on the immunohistochemical and clinicopathologic features (5–8).

In our study, 62.5% of the patients (5 of 8) showed ITPN with invasive carcinoma. This is similar to previous reports that up to 50% of ITPN cases are associated with invasive carcinoma (5, 8). Patients with invasive carcinoma showed a tendency to have larger tumor size and more main duct dilatation. This result is consistent with previous reports (1, 8). In addition, 3 of 5 cases of ITPN with invasive carcinoma were accompanied by pancreatoliths, whereas no cases of ITPN without invasive carcinoma had pancreatoliths. This might be because slowly growing intraductal tumors gradually obstruct the main pancreatic duct leading to insufficient drainage of pancreas juice and stone formation during the disease course transformed from high grade dysplasia to invasive carcinoma. Therefore, the presence of pancreatoliths in invasive ITPN can reflect the long disease course with less aggressive nature. This is also supported by the lack of stan-

dardized uptake value (SUV) and no diffusion restriction in the cases of invasive ITPN in our study.

The previous literature (10) suggested that the marked pancreatic duct dilatation caused by abundant mucin secretion in pancreatic IPMN could be a key imaging finding in the differential diagnosis from pancreatic ITPN with same intraductal tumor growth. However, our study results showed that marked pancreatic duct dilatation is also possible in ITPN with invasive carcinoma, which could be due to impacted pancreatoliths associated with a very slow-growing intraductal tumor. On the other hand, solid component in pancreatic IPMN rarely replaces the cyst or dilated main pancreatic duct even if it is in advanced state, whereas solid tumor in pancreatic ITPN tends to focally or diffusely occupy the dilated main pancreatic duct (10). This is possibly due to the fact that abundant mucin from IPMN replaces the pancreatic duct first rather than intraductal solid tumor. From our study, ITPN nearly replacing the pancreatic duct

was radiologically misdiagnosed as autoimmune pancreatitis or ductal adenocarcinoma instead of rare pancreatic ITPN.

Our case series demonstrated that EUS detected all intraductal solid tumors compared with CT or MRCP. The high resolution of EUS and close proximity to the target lesion of the pancreas could provide higher sensitivity for small solid tumors in the duct (11). However, CT or MRCP can provide additional information regarding the presence of synchronous biliary cancer, distant metastases, or concomitant chronic pancreatitis including pancreatoliths that assists diagnosis of pancreatic ITPN.

In our case series, half of the patients had synchronous or metachronous biliary cancer. Currently, there has been no report demonstrating the relationship between development of biliary cancers of different histologic type and pancreatic ITPN and further investigation is needed.

Pancreatic ITPN showed various imaging findings beyond the typical imaging findings of intraductal solid tumor, as reported in previous studies. In the present study, preoperative imaging diagnoses were chronic autoimmune pancreatitis, pancreatic ductal adenocarcinoma, or IPMN instead of pancreatic ITPN. Diffuse small intraductal tumors rendered the pancreatic duct dilatation irregular, mimicking autoimmune pancreatitis, and the solid component within the cystic mass of the pancreas led the radiologist to misdiagnose the malignant pancreatic IPMN on multimodality imaging. These various atypical imaging findings in addition to the rare disease incidence make it difficult for radiologists to achieve an imaging diagnosis for pancreatic ITPN (6, 12).

There are only two case reports of PET-CT study of pancreatic ITPN (13, 14). Our study showed varied ^{18}F-FDG uptake ranging from no to strong uptake in 4 patients regardless of invasive carcinoma component. Therefore, further study is required to determine the utility of PET-CT in patients with pancreatic ITPN.

There are several limitations to our study. First, this is a retrospective study of a small number of patients. Pancreatic ITPN is a very rare disease that has recently been categorized as one of the pancreatic intraductal neoplasms, so multicenter studies involving a large number of patients are needed to obtain accurate imaging information of this disease. Second, we did not compare pancreatic ITPN with pancreatic IPMN, which is its counterpart.

In conclusion, patients with associated invasive carcinoma from pancreatic ITPN may have presented a trend toward larger tumor size and dilated pancreatic duct with pancreatoliths, but the differences were not statistically significant. Further studies with a larger number of patients are needed to provide better insight into these findings. Pancreatic ITPN can show various atypical imaging findings as well as typical intraductal solid tumor on multimodality imaging. The presence of lesion multiplicity and synchronous or metachronous biliary cancer can be helpful for assisting with the diagnosis of pancreatic ITPN.

Conflict of interest disclosure
The authors declared no conflicts of interest.

References
1. Yamaguchi H, Shimizu M, Ban S, et al. Intraductal tubulopapillary neoplasms of the pancreas distinct from pancreatic intraepithelial neoplasia and intraductal papillary mucinous neoplasms. Am J Surg Pathol 2009; 33:1164–1172. [CrossRef]
2. Bosman FT CF, Hruba RH et al. WHO classification of tumours of the digestive system. 4th ed. IARC Press, Lyon, 2010; 304–313.
3. Yamaguchi H, Kuboki Y, Hatori T, et al. The discrete nature and distinguishing molecular features of pancreatic intraductal tubulopapillary neoplasms and intraductal papillary mucinous neoplasms of the gastric type, pyloric gland variant. J Pathol 2013; 231:335–341. [CrossRef]
4. Kloppel G, Basturk O, Schlitter AM, Konukiewitz B, Esposito I. Intraductal neoplasms of the pancreas. Semin Diagn Pathol 2014; 31:452–466. [CrossRef]
5. Rooney SL, Shi J. Intraductal tubulopapillary neoplasm of the pancreas: an update from a pathologist's perspective. Arch Pathol Lab Med 2016; 140:1068–1073. [CrossRef]
6. Date K, Okabayashi T, Shima Y, et al. Clinicopathological features and surgical outcomes of intraductal tubulopapillary neoplasm of the pancreas: a systematic review. Langenbecks. Arch Surg 2016; 401:439–447. [CrossRef]
7. Basturk O, Adsay V, Askan G, et al. Intraductal tubulopapillary neoplasm of the pancreas: a clinicopathologic and immunohistochemical analysis of 33 cases. Am J Surg Pathol 2016; 41:313–325. [CrossRef]
8. Kolby D, Thilen J, Andersson R, Sasor A, Ansari D. Multifocal intraductal tubulopapillary neoplasm of the pancreas with total pancreatectomy: report of a case and review of literature. Int J Clin Exp Pathol 2015; 8:9672–9680.
9. Chelliah A, Kalimuthu S, Chetty R. Intraductal tubular neoplasms of the pancreas: an overview. Ann Diagn Pathol 2016; 24:68–72. [CrossRef]
10. Motosugi U, Yamaguchi H, Furukawa T, et al. Imaging studies of intraductal tubulopapillary neoplasms of the pancreas: 2-tone duct sign and cork-of-wine-bottle sign as indicators of intraductal tumor growth. J Comput Assist Tomogr 2012; 36:710–717. [CrossRef]
11. Alkiviadis Efthymiou TP, and Emmanouil Zacharakis Endoscopic ultrasound in the diagnosis of pancreatic intraductal papillary mucinous neoplasms. World J Gastroenterol 2014; 20:7785–7793. [CrossRef]
12. Yoshida Y, Matsubayashi H, Sasaki K, Kanemoto H, Uesaka K, Ono H. Intraductal tubulopapillary neoplasm of the pancreatic branch duct showing atypical images. J Dig Dis 2015; 16:357–361. [CrossRef]
13. Someya Y, Nakamoto Y, Nakatani K, Kawaguchi M, Minamiguchi S, Togashi K. 18F-FDG uptake in intraductal tubulopapillary neoplasm of the pancreas. Clin Nucl Med 2014; 39:e277–280. [CrossRef]
14. Fujimoto Y, Tomimaru Y, Tamura H, et al. Pancreatic intraductal tubulopapillary neoplasm with associated invasive cancer successfully treated by total pancreatectomy: a case report. Oncol Lett 2017; 14:153–158. [CrossRef]